DECEMBER 1974 MATT-1085

MEASUREMENT OF THE DEVELOPMENT AND EVOLUTION OF SHOCK WAVES IN A LASER-INDUCED GAS BREAKDOWN PLASMA

BY

T. K. CHU AND L. C. JOHNSON

PLASMA PHYSICS LABORATORY

PRINCETON UNIVERSITY
PRINCETON, NEW JERSEY

This work was supported by U. S. Atomic Energy Commission Contract AT(11-1)-3073. Reproduction, translation, publication, use, and disposal, in whole or in part, by or for the United States Government is permitted.

DISCLAIMER

Measurement of the Development and Evolution of Shock Waves in a Laser-Induced Gas Breakdown Plasma

T. K. Chu and L. C. Johnson

Plasma Physics Laboratory, Princeton University

Princeton, New Jersey 08540 USA

ABSTRACT

Space- and time-resolved interferometric measurements of electron density in CO_2-laser produced plasmas in helium or hydrogen are made near the laser focal spot. Immediately after breakdown, a rapidly growing region of approximately uniform plasma density appears at the focal spot. After a few tens of nanoseconds, shock waves are formed, propagating both transverse and parallel to the incident laser beam direction. Behind the transverse propagating shock is an on-axis density minimum, which results in laser-beam self trapping. The shock wave propagating toward the focusing lens effectively shields the interior plasma from the incident beam, because the lower plasma temperature and higher plasma density in the shock allow strong absorption of the incident beam energy. By arranging the laser radiation-plasma interaction to begin at a plasma-vacuum interface at the exit of a free-expansion jet, this backward propagating shock wave is eliminated, thus permitting efficient energy deposition in the plasma interior.

I. INTRODUCTION

Interest has been growing in recent years in the possibility of utilizing CO_2 lasers for heating magnetically confined, weakly underdense fusion plasmas.[1-5] The configuration most frequently suggested is a linear device with a plasma column about 10^3 meters long, a few millimeters in diameter, confined radially by a magnetic field of several hundred kilogauss strength, and heated from the ends by powerful, long-pulse CO_2 lasers. The absorption length for 10.6 μm radiation in the heated plasma, if one assumes inverse bremsstrahlung to be the dominant mechanism, would be comparable to the length of the plasma column, and the beam would have to be refractively trapped by the column to allow efficient heating.

A number of papers have dealt with the refractive trapping of the beam by pre-existing radial plasma density distribution.[6-9] Measurements[10] and one-dimensional (radial) magnetohydrodynamic calculations[11] have also shown that favorable density profiles (with a density minimum on axis) arise within a few nanoseconds of laser absorption in a uniform neutral gas or cool plasma as a result of plasma expansion and the formation of radially propagating shock waves. Theoretical predictions[12] and observations[9] of filamentation due to thermal self-focusing have also been reported. A modest degree of heating of confined plasmas by CO_2 laser radiation has been observed in a number of experiments.[8,13-16]

The longitudinal growth of the heated region has received little attention because of theoretical and experimental difficulties. A bleaching wave, in which heating is so fast that

macroscopic plasma response may be neglected, was treated theoretically in a one-dimensional model by Rehm[17] and by Steinhauer and Ahlstrom.[18] Rehm[17] also showed numerically that, when the absorption length of the radiation is much less than the characteristic length of the plasma, the bleaching wave will become a laser-driven shock wave in a time of the order of the absorption length divided by the sound speed. Hoffman[14] has observed the longitudinal propagation of a heated region in an axially heated theta-pinch. This was interpreted as a bleaching wave resulting from the $T_e^{3/2}$ dependence of the inverse bremsstrahlung absorption length, although the evolution of electron density was not directly observed. Similarly, measurements of the growth of the luminous region in underdense, laser-induced gas breakdown plasmas[19,20] do not admit to a clear interpretation of the mode of propagation along the beam unless they are accompanied by space- and time-resolved plasma density measurements.

The present paper reports interferometric measurements of electron density in underdense hydrogen and helium plasmas produced by gas breakdown at the focal spot of a 30 J, 150 nsec FWHM, CO_2 laser. The temporal and spatial resolutions of the measurements (3 nsec and 50 μm, respectively) are sufficient to show the evolution of the electron density longitudinally as well as radially. Within 20 nsec after breakdown, a density minimum develops on axis, and density builds up behind shock waves propagating radially and in both longitudinal directions along the beam. The radially propagating wave becomes a cylindrical blast wave. The shock waves propagating longitudinally are laser-driven.

The backward-going wave partially shields the interior plasma and the forward-going wave, so that the relative speeds of the two laser-driven shock waves vary with plasma density. By positioning the focal plane of the laser in the steep gas pressure gradient of a free-expansion jet, the backward-going wave is eliminated, permitting efficient energy deposition in the downstream plasma. Some of these results have been briefly reported previously.[10,21]

II. EXPERIMENT

The experiment is shown schematically in Fig. 1. A 4-cm diameter, 0.3-mm thick diaphragm with a 5-mm diameter orifice separates and interconnects two chambers, one on each side of the focal plane. The downstream chamber is pulse-filled with a solenoid valve, while the upstream side is held under relative vacuum. The CO_2 laser is pulsed with a pre-set time delay relative to the time of valve opening, and gas pressure at the time of the laser pulse can be varied by adjusting this time delay. The gas pressure is monitored by measuring the fringe shift resulting from the gas pressure change, using the same Mach-Zehnder interferometer used for electron density measurement (described below). The laser pulse duration is $\sim 10^{-7}$ sec, the gas-pressure filling time is 10^{-2} sec, and its exit velocity at the orifice is $\sim 10^{4}$ cm/sec. Thus the gas can be considered as stationary both in space and time during the laser pulse duration, and has a steep axial gas density gradient across the laser beam focal plane. In experiments without the interface, the upstream valve is closed, the chambers are filled to the desired pressure, and the orifice may be removed.

The plasma is initiated at the focal spot of a TEA CO_2 laser with unstable resonator optics, which gives an annular output beam with 5-cm i.d. and 10-cm o.d., and beam divergence less than 1 mrad. The beam is focused by a KCl lens of 45 cm focal length. The radial intensity distribution at the focal plane is roughly Gaussian, with a measured focal spot diameter of less than 1 mm, approximately equal to that expected from spherical aberration. Photon drag detectors monitor the incident and transmitted beam. The central portion of the annular transmitted beam has negligible intensity when no plasma is present.

Electron density is measured side-on to the plasma with a He-Ne laser-illuminated Mach-Zehnder interferometer with photomultiplier detection.[10] A lens external to the interferometer focuses the beam of a 3 mW He-Ne laser to a diffraction limited spot in the plasma with a beam waist diameter of ~ 150 μm. The plasma region is then re-imaged at a photomultiplier which accepts a portion of the recombined beam corresponding to 50 μm in the plasma. Temporal resolution is limited by the photomultiplier (EMI 9785B) which has rise time of ~ 2 nsec. A mechanical shutter with a gate time of about a millisecond is used to prevent photomultiplier fatigue, and an interference filter blocks plasma luminosity at wavelength outside λ 632.8 ± 0.5 nm. The phase of the interferometer is adjusted to any desired value prior to the plasma formation by means of a piezoelectric translator on one of the mirrors. The photomultiplier then monitors the phase shift as a function of time, along the chord selected by the external optics, and the radial and longitudinal dependence is mapped by

shot-by-shot scanning. For most of the present measurements, the contribution of neutral gas immediately behind the shock fronts to the observed phase shift is negligible, so that one-wavelength interferometry is sufficient to establish the electron density unequivocally. The phase shift arising from the neutral gas along the 4 cm path through the discharge chamber during pulse-filling occurs on a millisecond time scale and may easily be distinguished from that due to the plasma formation and decay.

III. RESULTS

1. Radial Profiles

Typical plasma behavior for breakdown of ambient gas is shown in Fig. 2. The gas chamber, with the orifice removed, was filled with helium at an initial pressure of 30 torr. For complete double ionization and no hydrodynamic motion, this would give an electron density of 2×10^{18} cm^{-3}. The inset shows the luminous image at 50 nsec intervals beginning, with the bottom frame, approximately 10 nsec after breakdown. The plasma is viewed side-on, with the CO_2 laser beam propagating from left to right, and $z = 0$ represents the focal plane. At a given time, the luminous image is approximately cylindrical in shape, with a bright shell, and its length along the beam is several times its diameter.

The curves in Fig. 2 show electron density radial profiles in the focal plane at 10 nsec intervals for the first 100 nsec after breakdown. (These were obtained by Abel inversion of the fringe shift profiles.[22]) At 10 nsec the plasma profile is nearly rectangular, with a diameter somewhat larger than the beam waist

diameter. By 20 nsec there is already a deep minimum on axis, with density pile-up behind a radially expanding shock wave. At subsequent times, the central density continues to decrease as the plasma diameter increases. After 30 nsec the electron density maximum behind the shock wave begins to decrease as the wave slows down.

The evolution of electron density profiles in hydrogen is qualitatively the same as that for helium. Figure 3 shows corresponding profiles at 30 and 80 nsec after breakdown. The solid curves are for H_2 at 10 torr initial pressure, and the dashed curves are for He at 30 torr. Densities are lower for the hydrogen case, because of the lower filling pressure, and evolution is faster, because of the lower ion mass in the plasma and lower mass density ahead of the wave. Otherwise the two cases are quite similar and closely correspond with recent numerical solutions of one-dimensional magnetohydrodynamic equations for laser-induced heating and radial expansion of a cold, uniform hydrogen plasma.[11] It appears, therefore, that the hydrodynamic model, which assumes laser absorption by classical inverse bremsstrahlung, is essentially correct.

Time-resolved measurements of the intensity distribution of the CO_2 laser beam transmitted through the plasma[10] always show evidence of self-trapping of the beam. The precise character of the refracted beam intensity depends upong the opacity and length of the plasma along the beam as well as the density gradients transverse to the beam. An evaluation of the efficiency of self-trapping must await much more detailed measurements.

The radial propagation speed of the shock is highest immediately after breakdown and, after a few tens of nanoseconds, varies inversely with the shock radial position (plasma boundary). Figure 4 shows $r_o v_r$ vs. r_o for the two cases of Fig. 3, where r_o is the radial shock position and v_r is the shock speed. Curve a corresponds to helium at 30 torr, and curve b to hydrogen at 10 torr initial pressure. The asymptotic behavior ($r_o v_r$ = constant) is observed in both cases, and is characteristic of a cylindrical blast wave.[23]

A lower limit of laser energy deposition can be obtained from the propagation speed of the shock wave. Similarity solution of the hydrodynamic equations for a cylindrical blast wave[23] gives

$$r_o v_r = \frac{1}{2} (E_o/\rho_o \alpha)^{1/2} , \qquad (1)$$

where E_o is the "initial" energy input per unit length to the wave, ρ_o is the mass density ahead of the blast wave (6.6×10^{-6} gm/cm^3 for He at 30 torr, 1.1×10^{-6} gm/cm^3 for H_2 at 10 torr), and α is a numerical factor of order unity determined by the specific heat ratio γ of the hot-core plasma. If it is assumed that $\gamma = 5/4$, then

$$E_o = 2.1 \text{ J/cm} \quad \text{for He at 30 torr;}$$
$$E_o = 0.36 \text{ J/cm} \quad \text{for } H_2 \text{ at 10 torr.}$$

For $\gamma = 4/3$, the corresponding values are 1.6 and 0.27 J/cm, respectively.

These values of energy deposited are in qualitative agreement with absolute lower limits obtained by multiplying the maximum value of electrons per unit length in each case (from radial electron density profiles integrated over the plasma diameter) by the corresponding ionization potential. The values are 1 J/cm for helium and 0.2 J/cm for hydrogen.

From these estimates of energy per unit length, it is clear that relatively less energy is deposited in helium than the factor of 18 which would arise from the $Z_i n_e^2$ dependence of the inverse bremsstrahlung absorption coefficient. The explanation probably lies in a higher electron temperature and greater plasma opacity for the helium case.

2. Axial Profile and Beam Shielding

The measured variation along the beam axis of electron line density is shown in Fig. 5, at different times subsequent to breakdown at the focal plane ($z = 0$), for hydrogen plasma at 10 torr initial pressure. At less than 20 nsec, the profile is peaked at the focal plane, decreasing toward both edges. A gentle depression first appears in the profile slightly to the upstream of the focal plane at 20 nsec. At 30 nsec, a density pile-up has already developed on both the forward and the backward fronts. This density pile-up continues thereafter, stronger in the front running toward the focusing lens. Direct observation of the neutral gas shock wave is indicated in Fig.6, which shows the measured time change of fringe shift at $z = -2.25$ cm. The negative fringe shift preceeding the positive one due to the electron density increase results from the

increase of gas pressure ahead of the leading edge of the plasma, demonstrating neutral gas compression. It should be noted that these layers of neutral gas behind the shock waves become measurable only when their thickness and propagation speed fall within the limitations of the spatial and temporal resolutions of the present interferometric system, i.e., near the end of the laser pulse when the shock is greatly weakened and the ionization relaxation time therefore is increased.

Streak pictures of the longitudinal plasma expansion are shown in Fig. 7 for a series of initial hydrogen pressures. (The field of view for these pictures is $|Z| \lesssim 1.5$ cm). The laser beam is incident from the left. In general, there are two fronts, propagating in both directions along the beam. At very low pressure, the plasma is essentially transparent, and the available energy for absorption at the forward front is nearly the same as that at the backward front, resulting in almost symmetrical streak photographs. As pressure is increased, the plasma becomes less transparent, and more energy absorption results in faster propagation of both fronts. At still higher pressure, a substantial fraction of the beam intensity is absorbed in the backward propagating front, considerably reducing the intensity incident on the forward front, and resulting in unequal propagation speeds. Further increase of pressure essentially eliminates the forward propagating front.

Laser-driven luminous fronts in gas-breakdown plasmas have been the subject of numerous investigations, which will not be reviewed here. (A bibliographical review of work prior to 1969

was given by De Michelis.[24] References to more recent work, particularly that utilizing CO_2 lasers, may be found in a paper by Richardson and Alcock.[25]) Most of these experiments were concerned with breakdown of high pressure gases, for which the backward-propagating luminous front alone was present. Forward-going fronts were observed by Daiber and Thompson in an experiment with a ruby laser,[26] and by several authors using CO_2 lasers.[19-21,27] From all these investigations, it is clear that, in the case of laser-induced breakdown of ambient gas, a substantial fraction, if not all, of the incident intensity will be absorbed in the backward-going front. The present interferometric measurements show, in addition, that the electron density behind the longitudinally propagating, laser-driven fronts can exceed that in the plasma interior by a substantial margin, as a result of hydrodynamic motion. In order to efficiently heat a long, thin plasma column, the backward-propagating front must be eliminated.

3. Elimination of Backward-Propagating Shock Wave

Since a shock wave cannot propagate into a vacuum, its formation and propagation can be simultaneously eliminated at a plasma-vacuum interface. Such an interface can be made to occur near the exit of a free-expansion jet when the focal plane of the incident beam is positioned at the steep gas-density gradient across the exit. Plasma formation and heating therefore will begin at this plane. The scheme has been previously used by Thompson, Rehm, and Daiber in an experiment in overdense plasma to simulate laser-solid interactions.[28]

A streak picture of the free-expansion jet experiment, with the focal plane at the orifice exit, is shown in Fig. 8 for an initial hydrogen pressure of 10 torr. Again, the laser is incident from the left. The backward-propagating luminous front is no longer present. Similar results are observed for higher pressures. It has been also observed that, by moving the focal plane to the downstream of the orifice, a backward-propagating front will begin at the focal plane, toward the focusing lens, and abruptly stop at the interface. It should be noted that, during the laser pulse, the plasma diameter is less than the orifice diameter, and therefore no plasma-wall contact occurs.

Direct comparison of time-resolved electron line density at an upstream location z = -1.25 cm from the focal plane is shown in Fig. 9 for cases with and without the interface. Figure 9a shows the measured fringe shift as a function of time with a steady filling pressure of hydrogen at 10 torr. The plasma leading edge arrives at this location at 60 nsec after breakdown at the focal plane. The fringe shift increases rapidly to its peak value 1.15 in ~ 10 nsec and then immediately decreases. This rapid rise to, and fall from, the peak density is due to the passing of a thin layer of high density plasma behind the leading edge of the laser-driven shock wave. Figure 9b shows the corresponding plot in an experiment with the plasma-vacuum interface produced with the orifice arrangement. The pressure in the high pressure chamber is also 10 torr. The leading edge of the free-expansion plasma arrives at this location at ~ 345 nsec. The fringe shift rises slowly to a peak value of 0.043. The

sharp peak characterizing a shock wave is absent. Figure 10 shows the time of arrival of the plasma leading edge at various distances upstream from the focal plane for both cases. With the interface, curve b, the leading edge is greatly delayed. (The orifice arrangement during these measurements limited the access of the scanning He-Ne laser-illuminated interferometer to the plasma at distances greater than 12.5 mm from the focal plane.) We note that plasma formation with the forward propagating front, which has not been possible in high-density cases without the interface, has been observed at all densities with the present arrangement, indicating that energy deposition for heating purposes in the interior plasma is now possible.

IV. DISCUSSION

The present measurements clearly show the evolution of the electron density distribution in weakly underdense, laser-induced gas breakdown plasmas. Within 20 nsec after breakdown, the localized heating produces hydrodynamic motion which changes the initially uniform mass density distribution and leads to the development of shock waves propagating away from the focal spot. The radial plasma density profiles produced by the transverse hydrodynamic motion have on-axis minima and are favorable for the observed refractive trapping of the laser beam. The buildup of density behind the longitudinally-propagating waves results in a greater rate of energy absorption at the ends of the plasma column than in the plasma interior. By utilizing a free-expansion jet, the backward-propagating wave is eliminated so that the incident beam is not attenuated before reaching the focal plane.

These results have a number of important implications with reference to the proposed laser-heated reactor schemes.[1-5]

1) If a long plasma column is to be heated from the ends, ways must be found to efficiently couple the beam into the column. In particular, the gas pressure on the laser side of the focal plane must be low so that laser-driven absorption waves cannot propagate up the focusing cone and shield the plasma column from the beam. The free-expansion jet provides a simple, effective method of eliminating the cold plasma boundary layer at the end of the plasma column so that the beam may enter the column without severe attenuation.

2.) Transverse hydrodynamic motion, caused by localized energy deposition near the axis, will occur in a time of the order of the beam diameter divided by the sonic speed, i.e., within a few nanoseconds, after absorption begins at a given longitudinal position. This will result in plasma density profiles which are favorable for refractive trapping of the laser beam. It is not yet clear whether it will be necessary to establish a favorable profile before laser irradiation in order to permit heating of a long plasma column. It is clear, however, that any pre-existing density profile will be quickly altered by radial plasma motion, and it is the altered profile, rather than the initial one, that will govern the beam propagation at later times.

3.) Projected device lengths are so great that the time required for longitudinal growth of the heated region of the plasma column is quite substantial. (Even at the speed of light, the transit time is greater than a microsecond.) The mode of

propagation of the heating wave (bleaching wave, shock wave, etc.) will depend on the laser intensity at the wave front. This intensity will be determined by the transverse plasma motion,mentioned above, as well as by the laser power and the opacity of the plasma column. In order to adequately predict events in a reactor-size device, it will be necessary to construct a two-dimensional, self-consistent model in which the beam intensity, and hence the rate of absorption and the evolution of temperature and density profiles, is determined at each longitudinal position by refraction and absorption between that point and the laser.

This work was supported by the United States Atomic Energy Commission Contract AT(11-1)-3073.

REFERENCES

[1]J. M. Dawson, R. E. Kidder, and A. Hertzberg, Princeton Plasma Physics Laboratory Report MATT-782 (1971).

[2]J. M. Dawson, A. Hertzberg, R. E. Kidder, G. C. Vlases, H. G. Ahlstrom, and L. C. Steinhauer, in Fourth Conference on Plasma Physics and Controlled Fusion Research, (International Atomic Energy Agency, Vienna, 1971) Vol. I, p. 673.

[3]J. M. Dawson, W. L. Kruer, A. Hertzberg, G. C. Vlases, H. G. Ahlstrom, L. C. Steinhauer, and R. E. Kidder, Esfahan Symposium on Fundamental and Applied Science, (J. Wiley, New York, 1973), pp. 119-140.

[4]A. Hertzberg, AIAA 11th Aerospace Sciences Meeting, Washington D.C., January, 1973, AIAA Paper 73-258.

[5]W. R. Ellis and G. A. Sawyer, Los Alamos Scientific Laboratory Report, LA-5434-MS (1973).

[6]L. C. Steinhauer and H. G. Ahlstrom, Phys. Fluids 14, 1109 (1971).

[7]S. Humphries, Jr., Plasma Phys. 16, 623 (1974).

[8]N. A. Amherd and G. C. Vlases, Appl. Phys. Lett. 24, 93 (1974).

[9]G. M. Molen, M. Kristiansen, and M. O. Hagler, Appl. Phys. Lett. 23, 601 (1973).

[10]L. C. Johnson and T. K. Chu, Phys. Rev. Lett. 32, 517 (1974).

[11]N. H. Burnett and A. A. Offenberger, J. Appl. Phys. 45, 2155 (1974).

[12]F. W. Perkins and E. J. Valeo, Phys. Rev. Lett. 32, 1234 (1974).

[13]D. L. Jassby and M. E. Marhic, Phys. Rev. Lett. 29, 577 (1972).

[14]A. L. Hoffman, Appl. Phys. Lett. 23, 693 (1973).

[15]G. M. Molen, M. Kristiansen, M. O. Hagler, and R.D. Bengtson, Appl. Phys. Lett. 24, 583 (1974).

[16]R. Decoste, A. G. Engelhardt, V. Fuchs, and C. R. Neufeld, J. Appl. Phys. 45, 1127 (1974).

[17]R. Rehm, Phys. Fluids 13, 921 (1970).

[18]L. C. Steinhauer and H. G. Ahlstrom, Phys. Fluids 14, 81 (1971).

[19]N. H. Burnett and A. A. Offenberger, J. Appl. Phys. 45, 623 (1974).

[20]W. Halverson, Appl. Phys. Lett. 24, 364 (1974).

[21]T. K. Chu and L. C. Johnson, Bull. Am. Phys. Soc. 19, 642 (1974); also Fourth Annual Anomalous Absorption Conference, Lawrence Livermore Laboratory, Livermore, California (1974), paper B10.

[22]K. Bockasten, J. Opt. Soc. Amer. 51, 943 (1961).

[23]L. I. Sedov, Similarity and Dimensional Methods in Mechanics (Academic Press, New York, 1959), pp. 210-251.

[24]C. De Michelis, IEEE J. Quantum Electron. QE-5, 188 (1969).

[25]M. C. Richardson and A. J. Alcock, IEEE J. Quantum Electron. QE-9, 1139 (1973).

[26]J. W. Daiber and H. M. Thompson, Phys. Fluids 10, 1162 (1967).

[27]T. K. Chu and L. C. Johnson, Bull. Am. Phys. Soc. 18, 1325 (1973); L. C. Johnson and T. K. Chu, Bull. Am. Phys. Soc. 18, 1325 (1973).

[28]H. M. Thompson, R. G. Rehm, and J. W. Daiber, J. Appl. Phys. 42, 310 (1971).

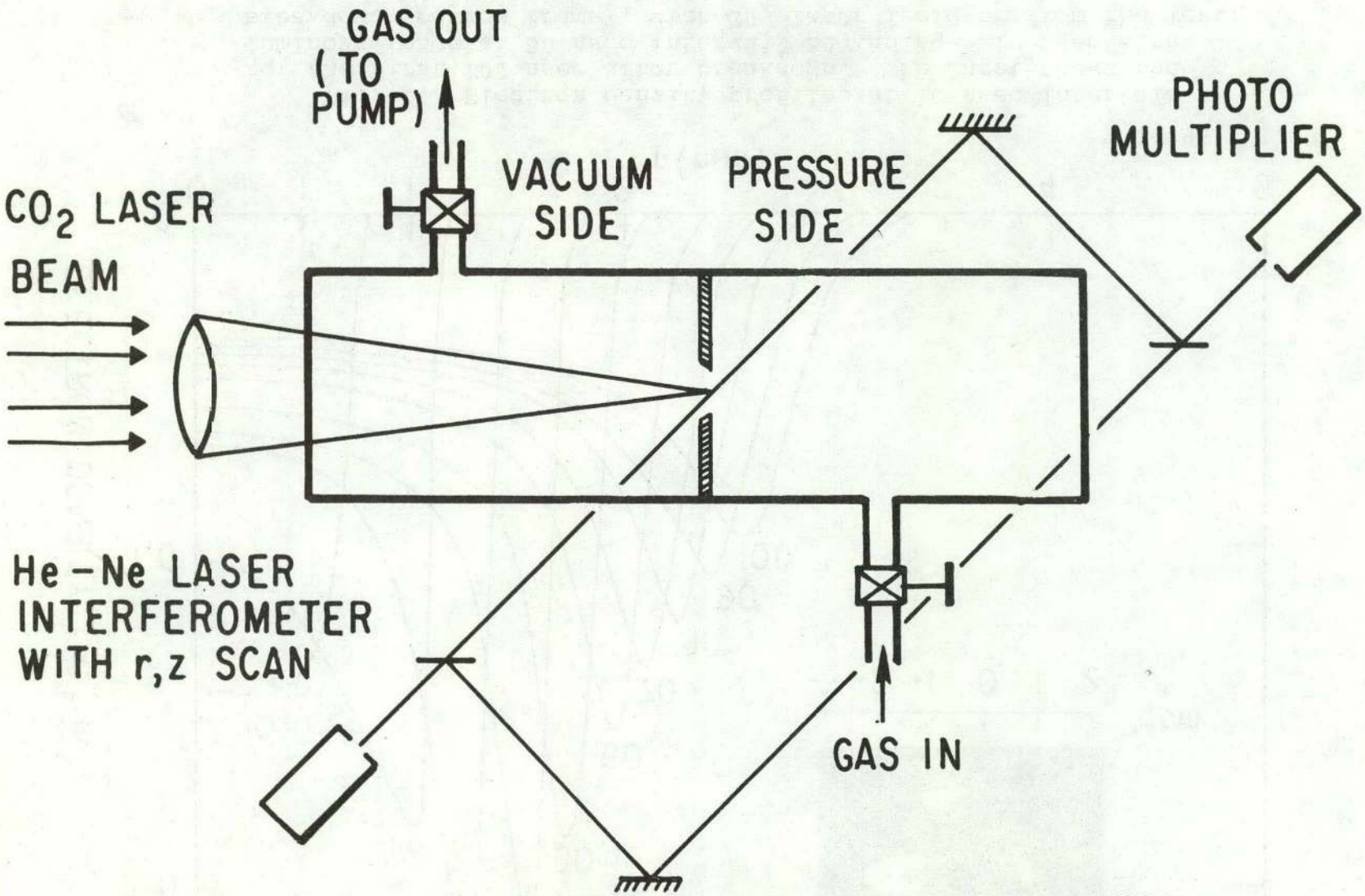

Fig. 1. Schematic of test section. A steep gas pressure gradient is established at the exit of the orifice when the pressure side is pulse-filled just prior to laser pulse. In experiments without the steep-gradient interface, the entire chamber is filled to desired pressure and the orifice may be removed.

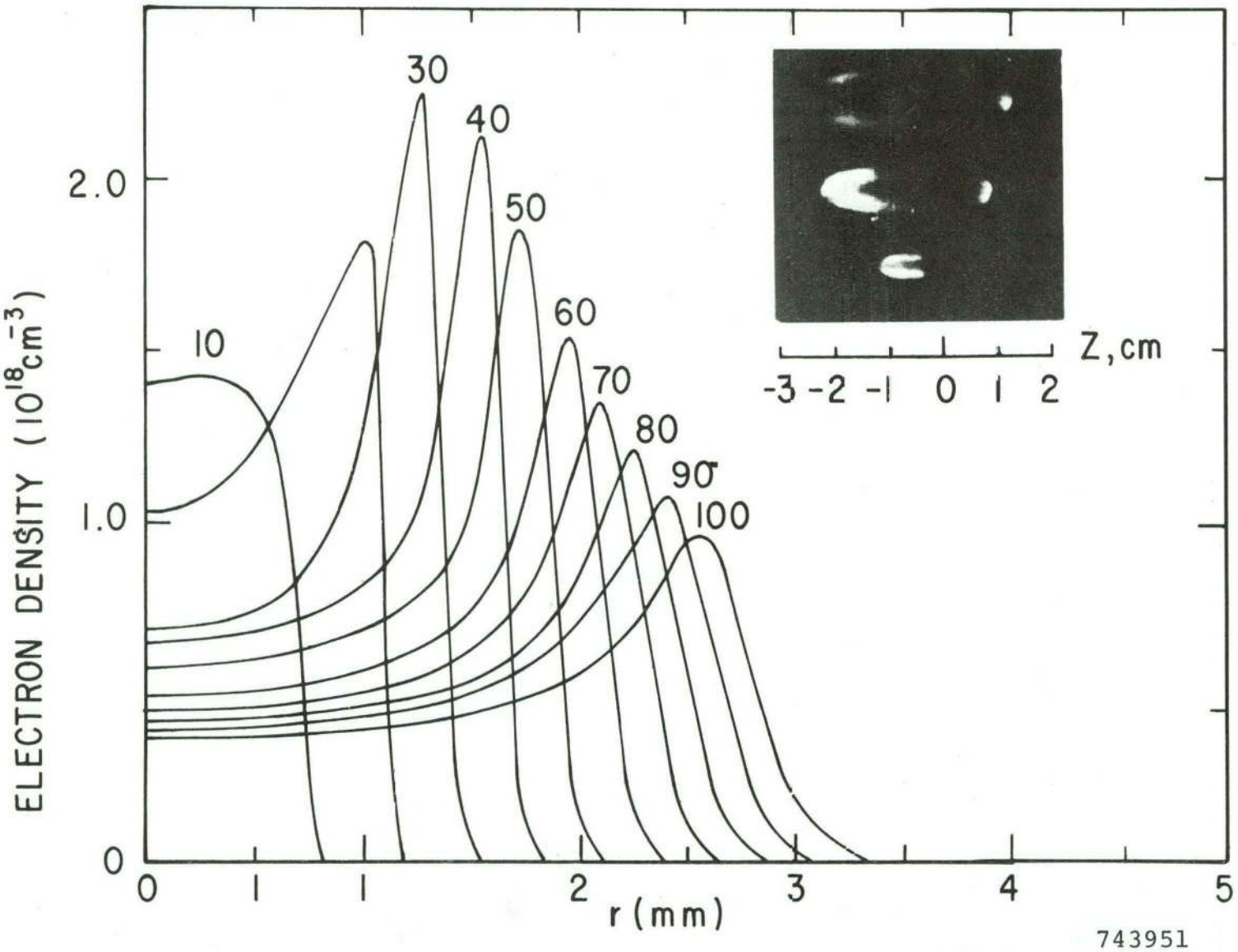

Fig. 2. Electron density profiles at 10 nsec intervals for the first 100 nsec after breakdown. The inset shows the luminous image at 50 nsec intervals beginning ~ 10 nsec after breakdown (bottom frame), with CO_2 laser incident from the left. He plasma, initial pressure 30 torr.

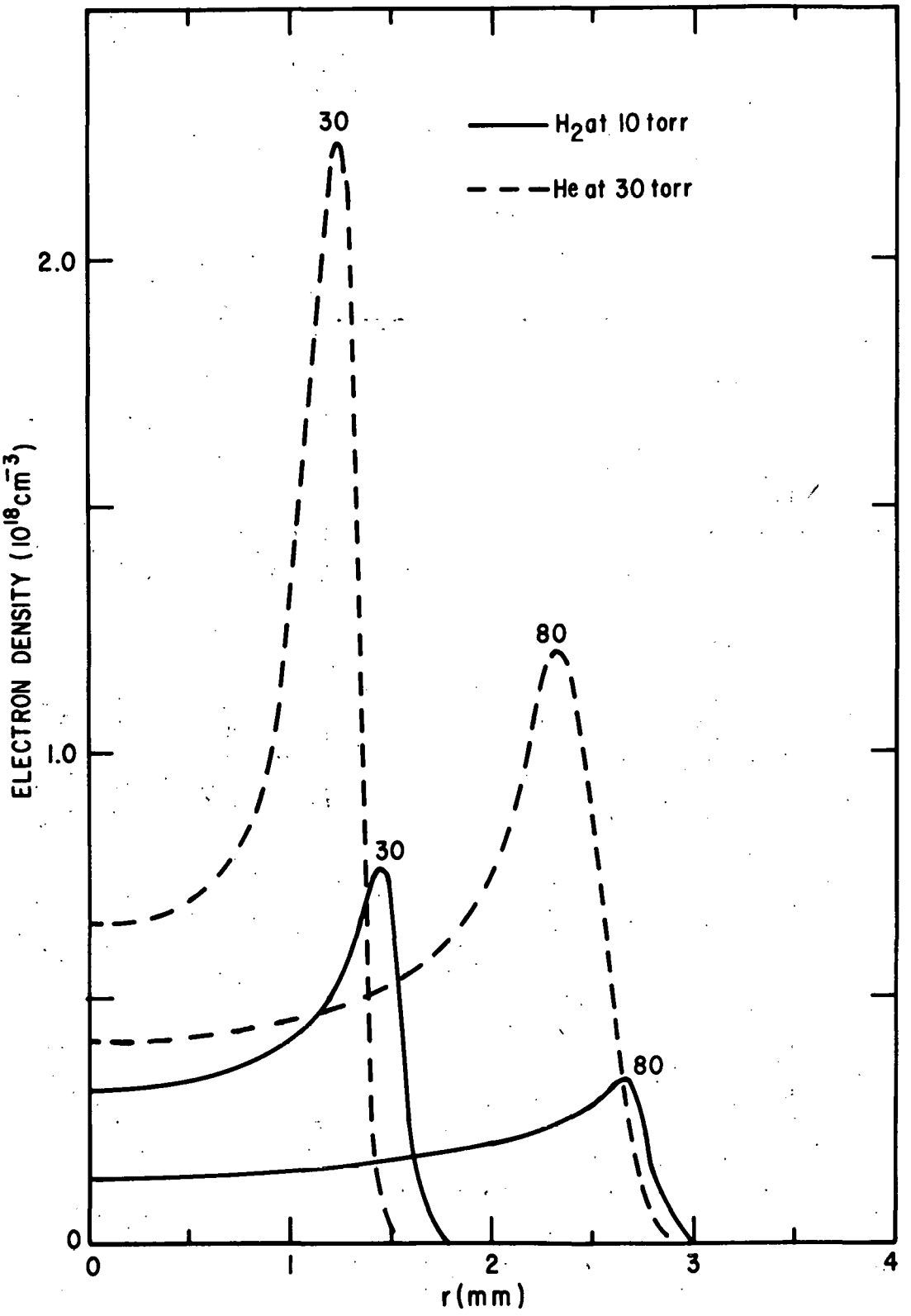

Fig. 3. Electron density profiles at 30 and 80 nsec after breakdown for hydrogen (initial pressure 10 torr) and helium (initial pressure 30 torr) plasmas.

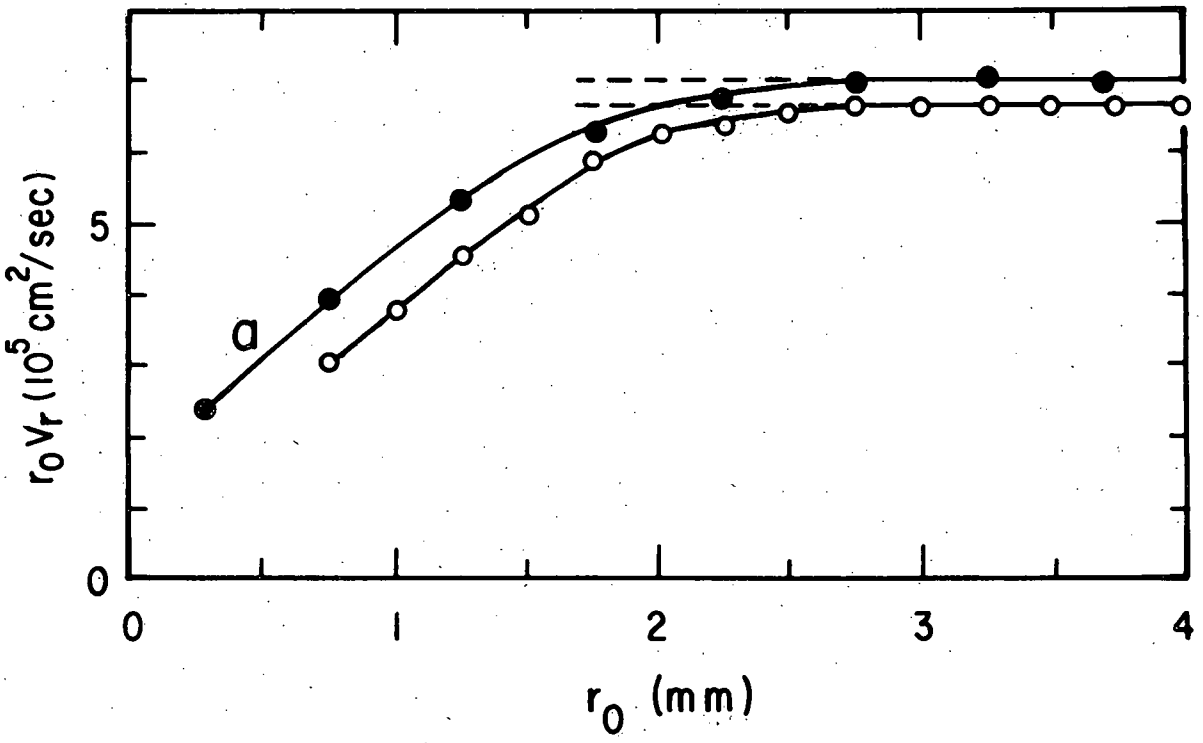

743948

Fig. 4. $r_o v_r$ versus r_o, where r_o is the shock position and v_r is the shock speed. Plasma parameters are the same as those of Fig. 3. The dashed lines are according to theory for cylindrical blast wave with an "initial" energy input.

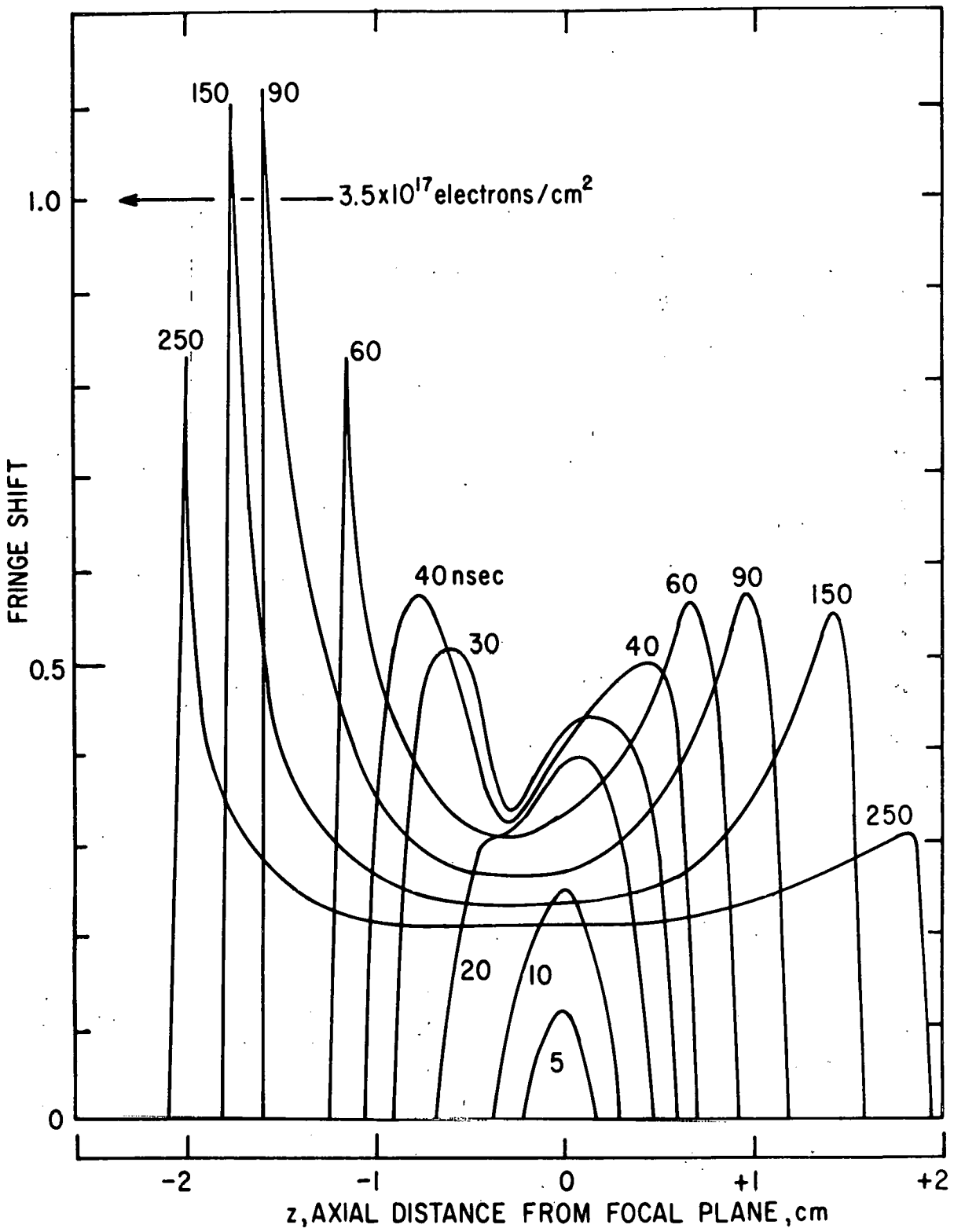

Fig. 5. Longitudinal distribution of on-axis fring shift. The time shonw in each curve, in nanoseconds, is referenced to the time of breakdown at the focal plane, z = 0.

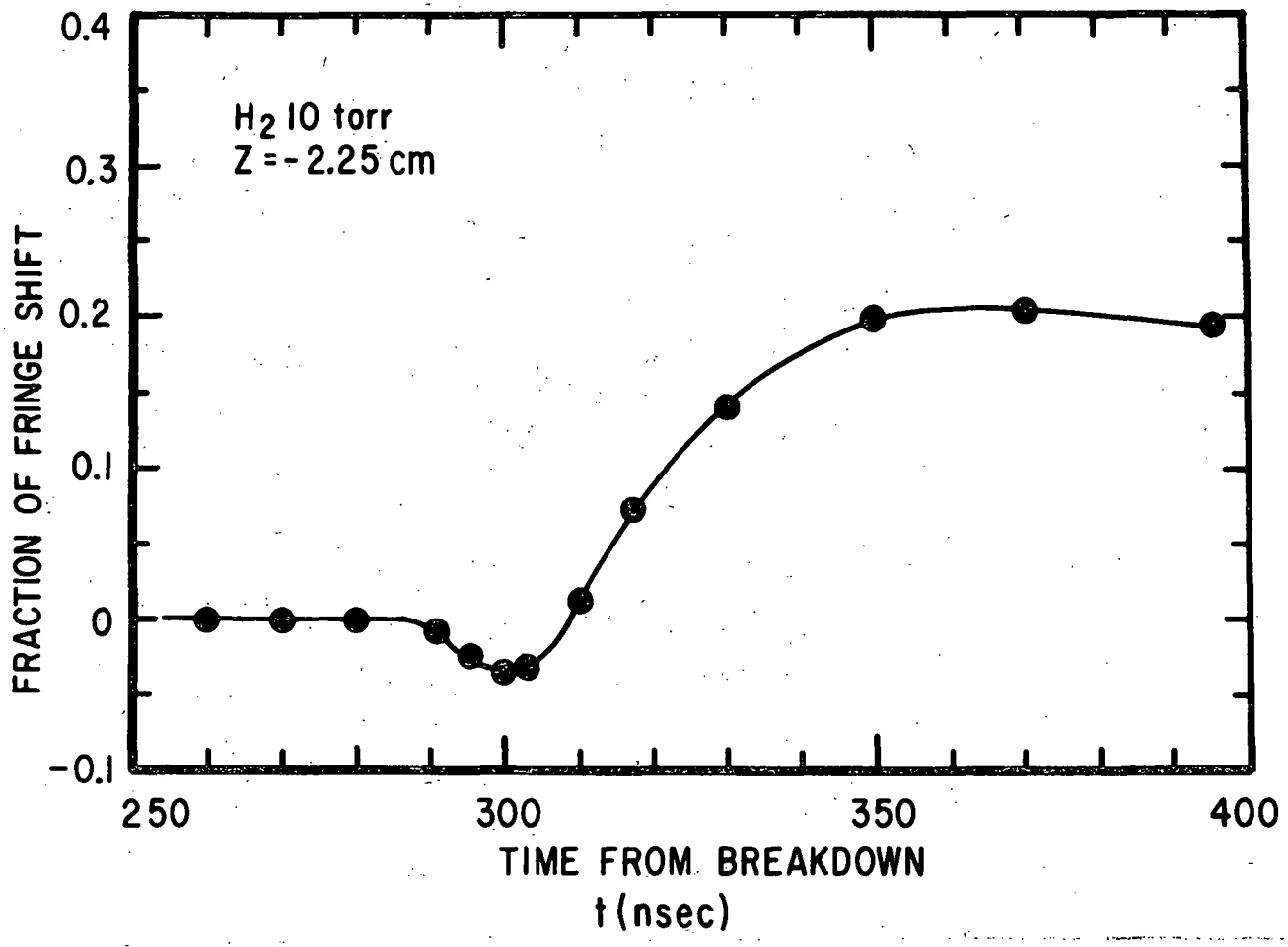

743950

Fig. 6. Fringe shift versus time at z = -2.25 cm. The negative shift preceeding the positive shift (due to electron density increase) is due to the compressed neutral gas. H_2 at 10 torr.

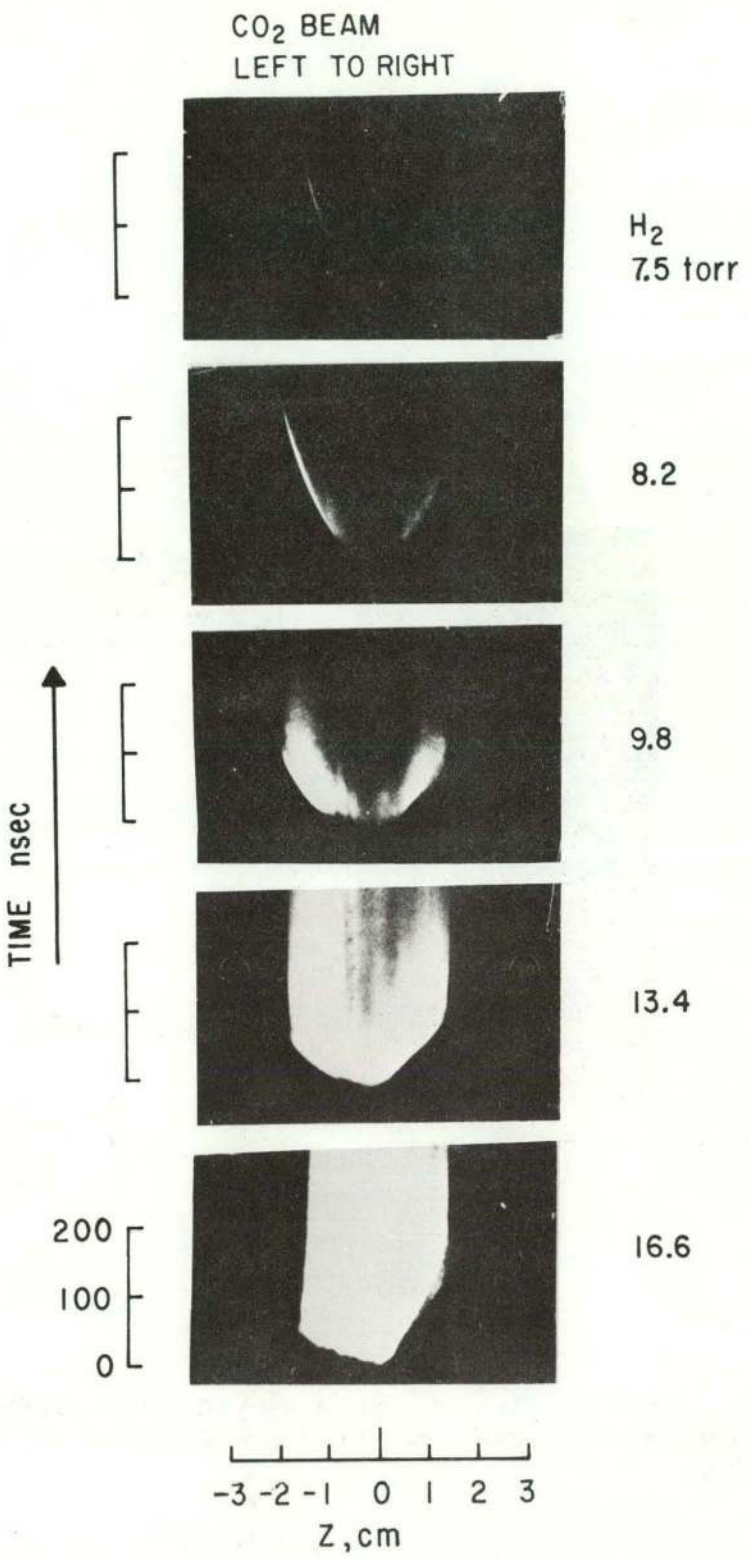

Fig. 7. Streak pictures showing longitudinal propagation of plasma luminous front (backward and forward) when the (hydrogen) neutral pressure is varied. Field of view is $|Z| \lesssim 1.5$ cm.

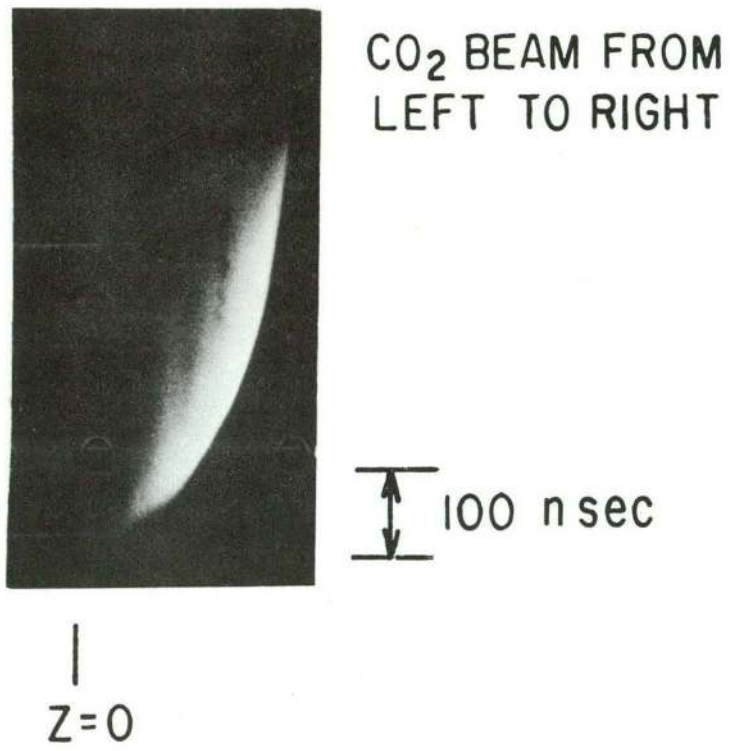

743993

Fig. 8. Streak picture showing the elimination of the backward propagating luminous front. (Z scale is not calibrated). H_2 at 10 torr.

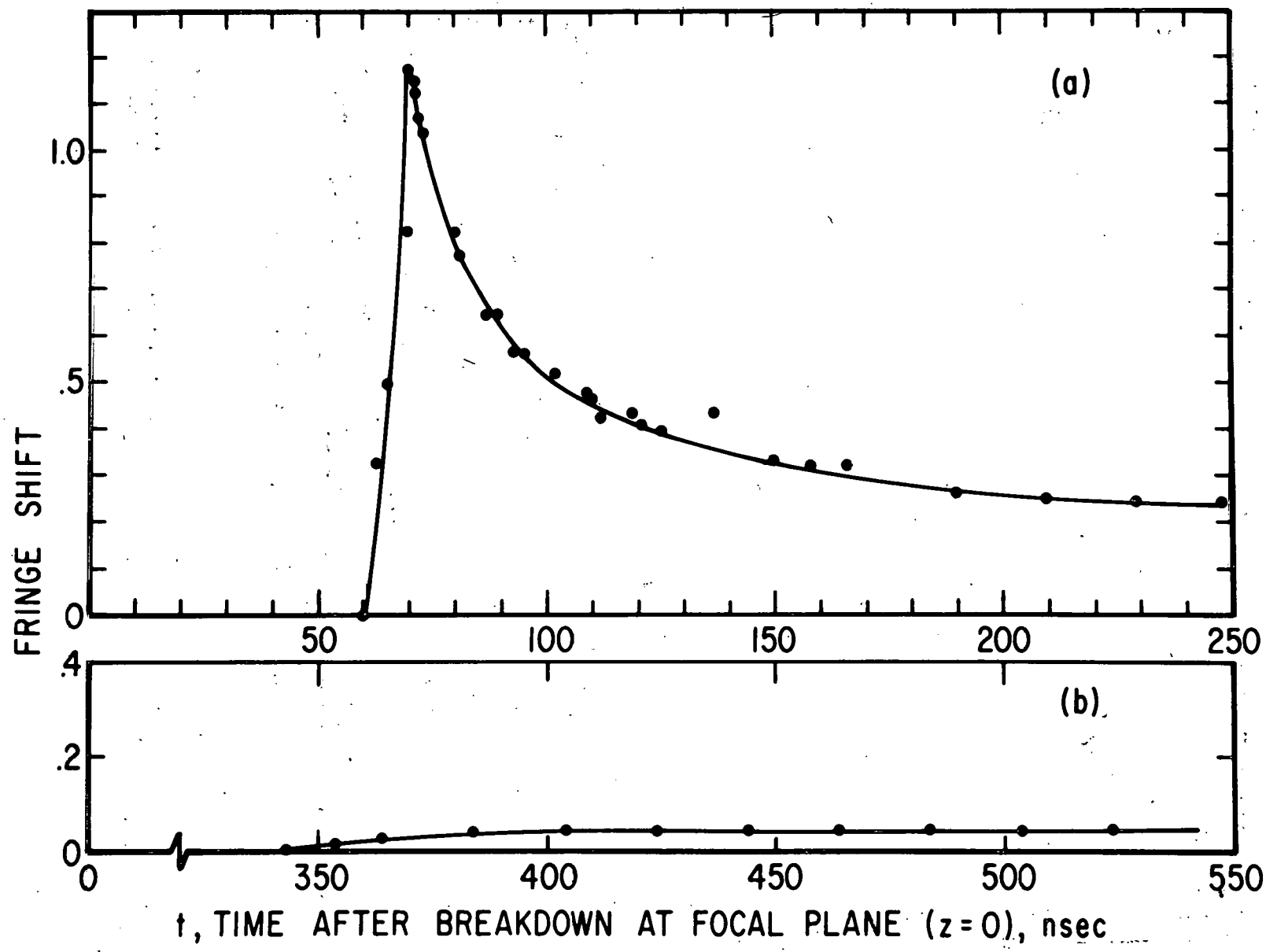

Fig. 9. Fringe shift versus time at Z = -1.25 cm. (a) Without the interface. (b) With the interface. H_2 at 10 torr.

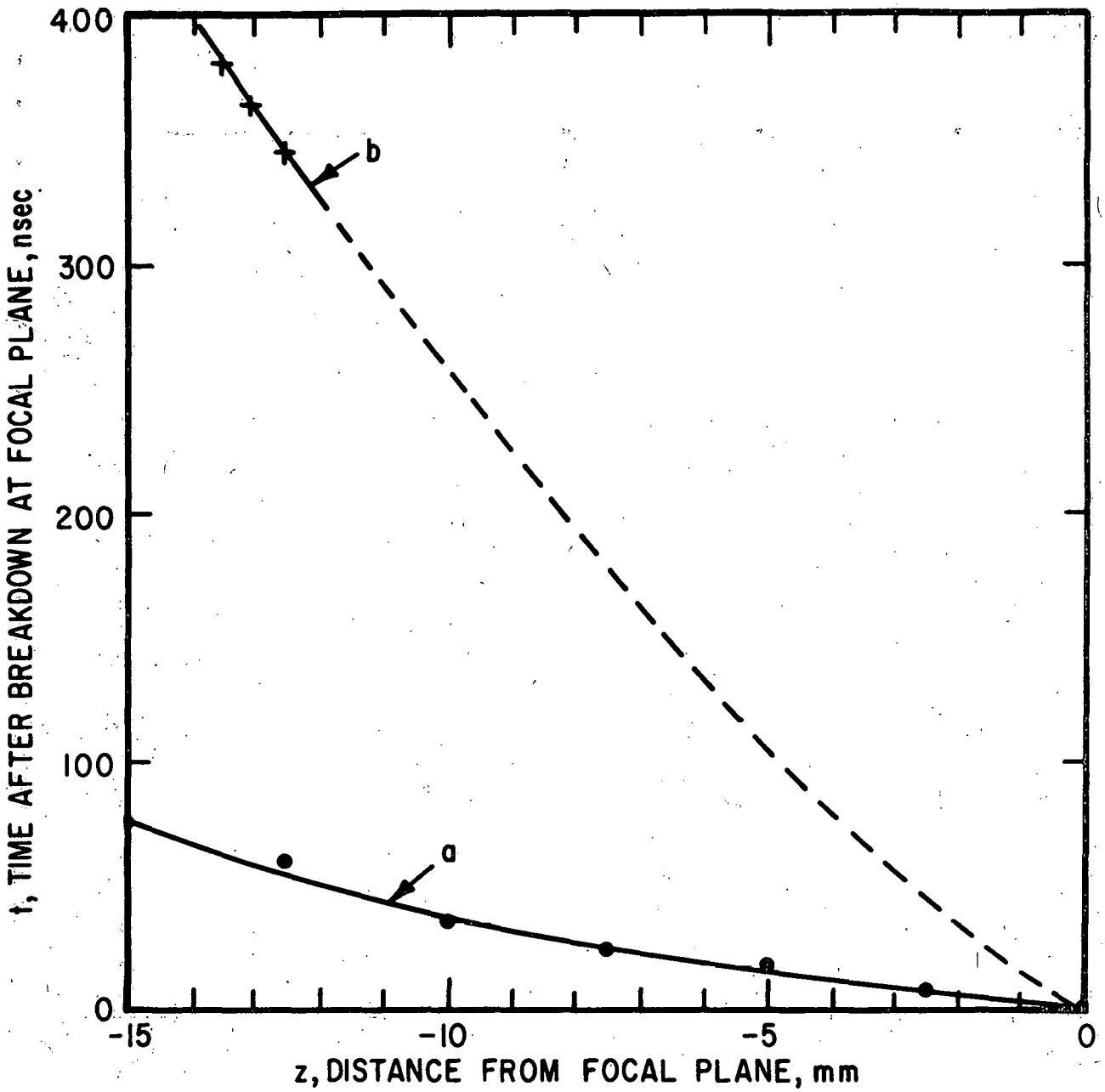

Fig. 10. Arrival time of the plasma leading edge at various upstream (Z < 0) locations. Curve a, without interface; curve b with interface. H_2 at 10 torr.